Available online at www.sciencedirect.com

SCIENCE DIRECT®

Nuclear Instruments and Methods in Physics Research A 544 (2005) 659–667

NUCLEAR INSTRUMENTS & METHODS IN PHYSICS RESEARCH Section A

www.elsevier.com/locate/nima

Minimizing the statistical error in capture cross-section measurements

Yaron Danon*, Robert C. Block

Department of Mechanical Aerospace and Nuclear Engineering, Rensselaer Polytechnic Institute, NES Bldg., 110 8th St., Troy, NY 12180, USA

Received 28 September 2004; received in revised form 2 December 2004; accepted 16 December 2004
Available online 5 March 2005

Abstract

Measurements of the neutron capture cross-section are performed by measurement of the capture rate of a sample placed in a neutron beam. The capture rate is measured by surrounding the sample with gamma-ray detectors. The capture rate is corrected for background and divided by the rate of neutrons incident on the sample in order to obtain the capture yield. The neutron capture cross-section can be obtained from the capture yield if additional information such as the total or scattering cross-section is known. An error analysis was performed on the measured capture cross-section. The error was minimized with respect to the experimental time split of the capture, background and incident neutron rates and also with respect to the sample thickness. These calculations are useful for the planning of an efficient capture cross-section experiment. The derived equations are compared to experimental data and show excellent agreement. This type of error analysis and minimization is also valid for other types of partial cross-section measurements such as fission and scattering which have similar expressions for the measured yield.

PACS: 25.40.Ny; 25.60.Dz; 29.30.Hs

Keywords: Cross-section; Capture; Transmission; Counting statistics; Error analysis

1. Introduction

Neutron capture and transmission experiments can provide information about the neutron induced capture and total cross-sections. In addition, when performed in the resonance region these measurements provide information about the resonance parameters. In previous work [1], we described methods to minimize the statistical uncertainty of total cross-section measurements and the derived resonance parameters. In this work, we would like to extend the analysis to

*Corresponding author. Tel.: +518 276 4008; fax: +518 276 4832.
E-mail address: danony@rpi.edu (Y. Danon).

0168-9002/$ - see front matter
doi:10.1016/j.nima.2004.12.034

capture cross-section measurements. Previous work on similar experiment optimization was done by Rose and Shapiro [2] and dealt only with transmission measurements and was later extended to resonance parameters in Ref. [1].

A capture cross-section measurement is typically done using the time-of-flight (TOF) method or thermal beams from reactors. In such a measurement, the sample is placed in a neutron beam and the gamma-rays resulting from capture reactions in the sample are recorded by detectors surrounding the sample. Consider geometry similar to the RPI capture detector [3] shown in Fig. 1. The number of capture interactions in the sample is given by the sum of first collision events plus multiple scattering events. The number of first collision capture events per incident neutron or the capture yield Y, at a given neutron energy is given by

$$Y = (1 - \exp(-N\sigma_t))(1 - \xi) \quad (1)$$

where N is the sample number density (atoms/barn), σ_t is the total cross-section which is a sum of the capture cross-section σ_γ and the scattering cross-section σ_s and ξ is the scattering fraction $\xi = \sigma_s/\sigma_t$ $(0 \leqslant \xi < 1)$. This assumes a typical case where the reaction includes capture and scattering only such that $\sigma_t = \sigma_\gamma + \sigma_s$. Multiple scattering events are a function of the scattering cross-section, and as the scattering increases, the number of captures in the sample will also increase. For the purpose and simplicity of this analysis, the multiple scattering is assumed to be a small effect and is ignored.

For a capture experiment, the detector capture rate r_γ (neglecting multiple scattering) is given by

$$r_\gamma = r_\phi k(1 - \exp(-N\sigma_t))(1 - \xi) + r_b \quad (2)$$

where r_ϕ is the incident neutron rate, r_b is the background rate, and k is the gamma-ray detection efficiency. It is assumed that the absorption of gammas in the sample is small and was ignored. A typical capture experiment involves three separate measurements; one to measure the capture rate r_γ, the second to measure the incident neutron rate r_ϕ, and the third to measure the capture background rate r_b. A normalization factor is often used in order to take into account the detector efficiency and the relative measurement of the incident neutron rate, in such case k also represent this factor. Thus an expression for the measured capture yield is given by

$$Y = \frac{r_\gamma - r_b}{k r_\phi}. \quad (3)$$

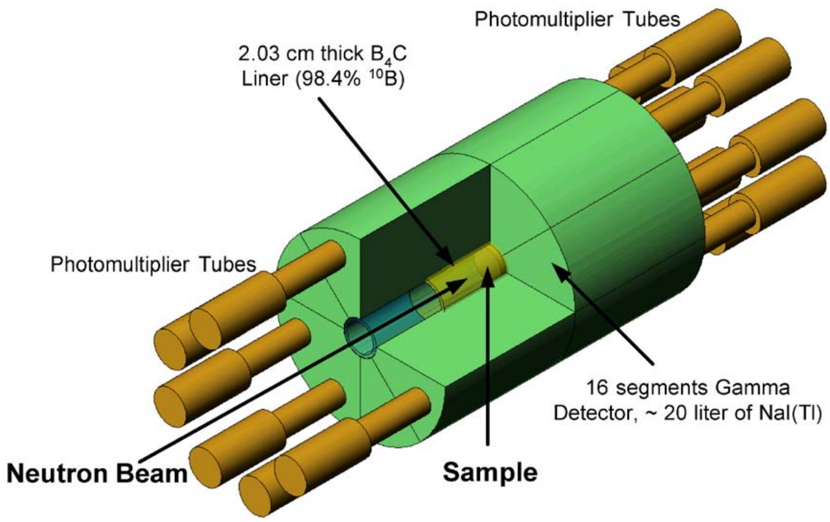

Fig. 1. The RPI capture detector in which the sample is in the center of a 16 segment hallow cylindrical NaI(Tl) detector. The sample is surrounded by a $^{10}B_4C$ liner that absorbs scattered neutrons in order to reduce the background from neutron capture in iodine (more details in Ref. [3]).

In TOF capture measurements, the incident-neutron-rate shape as function of neutron energy is also measured. The incident-neutron-rate measurement can be done in different ways, for example, using a strong ^{10}B enriched absorber in the same configuration at shown in Fig. 1 (see, for example, Ref. [4]). Although this neutron rate measurement might involve a background measurement, the background is less important because the count rate from the boron sample is typically higher than the rate from the sample.

A measurement of the capture yield Y can be translated to a measurement of the capture cross-section by solving Eq. (1) for σ_γ and applying the relation $\sigma_\gamma = \sigma_t(1-\xi)$;

$$\sigma_\gamma = -\frac{(1-\xi)}{N}\ln\left(1-\frac{Y}{1-\xi}\right). \tag{4}$$

Thus, in order to obtain the capture cross-section from such a measurement, additional information about the scattering cross-section is required; such information can be obtained from a total cross-section (transmission experiments) or a scattering measurement. For a "pure" capture sample ($\xi = 0$), the capture measurement alone is sufficient to determine the capture cross-section directly. What is important to note is that the accuracy in σ_γ is determined by the accuracy of the measured capture yield Y which is given by Eq. (3).

Ignoring for a moment the counting statistical errors in r_ϕ and r_b, the capture yield Y given in Eq. (3) is linear with respect to the capture rate r_γ, indicating that if the capture rate r_γ is larger, the capture yield Y will increase and the counting statistical error in Y will decrease. Thus, there is an incentive to make such a measurement with a thick sample. However, a thick sample might cause a problem with increased multiple scattering that has to be corrected for. Fitting codes such as SAMMY [5] and REFIT [6] include very good algorithms to perform such corrections. In the case of very thick samples, there might also be a problem of gamma absorption in the sample itself which will lower the observed yield and require a correction in order to obtain accurate cross-sections. In some cases, the sample thickness is limited to the amount of material available, or in the case of unstable isotopes the activity of the sample which increases the background rate.

The next question is then; how thick should the sample be? It is clear that if the sample is made too thick the capture yield will be $Y = 1-\xi$ and thus Eq. (2) becomes a measurement of the incident neuron rate times the ratio of capture to total cross-section or for a pure capture sample a measurement of the incident neutron rate. On the other hand, if the sample is too thin the measured capture rate r_γ will be small and will have a large statistical uncertainty associated with it. Thus, there must be an optimal sample thickness (or capture yield) that will minimize the uncertainty due to counting statistics.

The purpose of this work is to perform an analysis that will show the relationship between the fractional error of the capture cross-section and that of the measured capture yield. An optimized expression for splitting a given experiment time to capture, background and incident neutron rate measurements will be a derivative of this work. This type of analysis can provide guidelines for sample thickness selection and capture experiments design. This type of analysis can also be applied for other partial cross-section measurements such as fission and scattering where the expression for the measured yield is similar to Eq. (1).

The analysis shown here relates to the capture cross-section itself. We also restrict this analysis to a case of a constant capture cross-section. An interesting extension of this work would be to find the relationship between the errors of the measured resonance parameters and that of capture yield. This topic will be the subject of a future publication and will not be presented here; however, similar work for transmission experiments was given in Ref. [1].

2. Error analysis

In order to minimize the error in the capture cross-section, an error propagation approach is used. The errors included in this analysis are strictly from counting statistics and for simplicity, any possible correlation between measured quantities is ignored.

The squared fractional error in the capture cross-section as given by Eq. (4) is obtained by simple error propagation

$$\left(\frac{\Delta\sigma_\gamma}{\sigma_\gamma}\right)^2 = \left(\frac{\partial\sigma_\gamma}{\partial Y}\frac{\Delta Y}{\sigma_\gamma}\right)^2 \tag{5}$$

where $\Delta\sigma_\gamma$ and ΔY are the counting statistics error in the capture cross-section and capture yield,respectively. Taking the derivative of the capture yield given in Eq. (1), gives

$$\left(\frac{\Delta\sigma_\gamma}{\sigma_\gamma}\right)^2 = \frac{1}{(N\sigma_t(1-\xi))^2}\left(\frac{\Delta Y}{(1-Y)/(1-\xi)}\right)^2. \tag{6}$$

The error in the capture yield can be calculated by propagating the counting statistics error of all the quantities in Eq. (3):

$$\Delta Y^2 = \left(\frac{\partial Y}{\partial r_\gamma}\Delta r_\gamma\right)^2 + \left(\frac{\partial Y}{\partial r_b}\Delta r_b\right)^2 + \left(\frac{\partial Y}{\partial r_\phi}\Delta r_\phi\right)^2. \tag{7}$$

We note the total experiment time as t which is equal to the sum of the time required to perform the three measurements of the capture, background and incident neutron rates (labeled as r_γ, r_b and r_ϕ, respectively) thus $t = t_\gamma + t_b + t_\phi$. The squared statistical error in each of the rates is given by $\Delta r_\gamma^2 = r_\gamma/t_\gamma$, $\Delta r_b^2 = r_b/t_b$ and $\Delta r_\phi^2 = r_\phi/t_\phi$. Substituting these values and calculating the derivatives, Eq. (6) becomes

$$\left(\frac{\Delta\sigma_\gamma}{\sigma_\gamma}\right)^2 = \frac{1}{(1-\xi)^2 x^2((1-Y)/(1-\xi))^2}\frac{1}{(kr_\phi)^2} \times\left[\frac{r_\gamma}{t_\gamma}+\frac{r_b}{t_b}+\left(\frac{r_\gamma - r_b}{r_\phi}\right)^2\frac{r_\phi}{t_\phi}\right] \tag{8}$$

where x is the optical thickness of the sample ($x \equiv N\sigma_t$). The background-to-signal ratio m is defined as

$$m \equiv \frac{r_b}{kr_\phi - r_b}. \tag{9}$$

Using Eqs. (8) and (9) and defining the fractional time for each of the capture, background and incident neutron rate measurements as $\alpha_\gamma = t_\gamma/t$, $\alpha_b = t_b/t$ and $\alpha_\phi = t_\phi/t$, respectively. The following expression for the squared fractional error in the capture cross-section can be derived:

$$\left(\frac{\Delta\sigma_\gamma}{\sigma_\gamma}\right)^2 = \frac{1}{tkr_\phi(1-\xi)^2}\frac{1}{x^2((1-Y)/(1-\xi))^2} \times\left[\frac{f_\gamma^2}{\alpha_\gamma}+\frac{f_b^2}{\alpha_b}+\frac{f_\phi^2}{\alpha_\phi}\right] \tag{10}$$

where

$$f_\gamma^2 = \left(Y + \frac{m}{m+1}\right),\quad f_b^2 = \frac{m}{m+1}\ \text{and}\ f_\phi^2 = kY^2.$$

A minimization procedure similar to the one used in Refs. [1,2] can now be applied. The objective is to minimize Eq. (10) with respect to α_γ, α_b and α_ϕ with the restriction that $\alpha_\gamma + \alpha_b + \alpha_\phi = 1$. The result for the optimum time split is given by

$\alpha_\gamma = f_\gamma/(f_\gamma + f_b + f_\phi)$, $\alpha_b = f_b/(f_\gamma + f_b + f_\phi)$ and $\alpha_\phi = f_\phi/(f_\gamma + f_b + f_\phi)$. Inserting these values to Eq. (10) gives

$$\left(\frac{\Delta\sigma_\gamma}{\sigma_\gamma}\right)^2_{\text{opt}} = \frac{1}{tkr_\phi(1-\xi)^2}\frac{1}{x^2(1-Y/1-\xi)^2} \times\left[f_\gamma + f_b + f_\phi\right]^2. \tag{11}$$

Substitution of equation (1) to equation (11) provide an expression for the minimum squared fraction error in the capture cross-section as a function of the optical thickness x:

$$\left(\frac{\Delta\sigma_\gamma}{\sigma_\gamma}\right)^2_{\text{opt}} = \frac{1}{tkr_\phi(1-\xi)^2}\frac{1}{x^2\exp(-2x)} \times\left[\sqrt{(1-\exp(-x))(1-\xi)+\frac{m}{m+1}} + \sqrt{\frac{m}{m+1}} + \sqrt{k}(1-\exp(-x))(1-\xi)\right]^2. \tag{12}$$

This equation can be numerically minimized with respect to x to find the optimum thickness of the sample as a function of the background-to-signal ratio m and the ratio of scattering fraction ξ. Notice that the term $1/tkr_\phi(1-\xi)^2$ in Eq. (12) is a constant and does not affect the minimization procedure. Also note that if the incident neutron rate r_ϕ is measured to much higher accuracy than the capture rate, it can be eliminated from the procedure by removing the last term in the square brackets. Similarly the error due to the background rate r_b can be eliminated by setting $m = 0$.

It is also interesting to note that although the capture cross-section is a complicated function of the reaction rates, the fractional error in the capture cross-section is inversely proportional to the square root of the total experiment time t.

3. Results

The derived equations can provide some information about the sample thickness or capture yield required to measure the capture cross-section while minimizing the uncertainty due to counting statistics. To demonstrate such a calculation, Eq. (12) was numerically minimized with respect to x. The calculations were done for several values of the scattering fraction ξ, and for a representative value of the normalization factor $k = 1$. The capture yield calculated using Eq. (1) for the optimal thickness is plotted as a function of the background-to-signal ratio in Fig. 2.

The solid line curve in Fig. 2 is for a pure capture sample. Regardless of the background-to-signal ratio, the optimum capture yield is bounded between 0.37 and 0.56. As expected, the optimum yield increases as the background increases. The dependence of the optimum yield on the scattering fraction ξ might seem confusing; observing Eq. (2), an increase in the scattering fraction ξ will result in reduction in the count rate and thus a thicker sample is required in order to increase the rate and reduce the error. However, Fig. 2 shows that an increase in the scattering fraction reduces the optimum yield. To further investigate this, Fig. 3 shows the same data plotted with respect to background-to-signal ratio m. This plot indicates that indeed, as expected, as ξ increases, the sample thickness also increases.

An investigation of the changes in the fractional error of the capture cross-section as a function of the sample yield and the background-to-signal ratio is shown is Figs. 4 and 5. Fig. 4 shows a calculation for a pure capture sample ($\xi = 0$) with $k = 1$. As indicated by the results plotted in Fig. 2, the optimum yield is in the same range of $Y = 0.37-0.56$. A deviation from the optimum yield will result in an increase in the fractional error of the measured capture cross-section, for example, for a background-to-signal ratio $m = 1/100$ and a

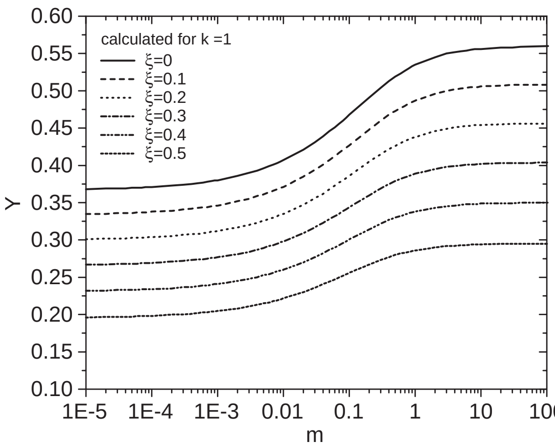

Fig. 2. Optimal capture yield Y as a function of the background-to-signal ratio m calculated for different values of the scattering fraction ξ.

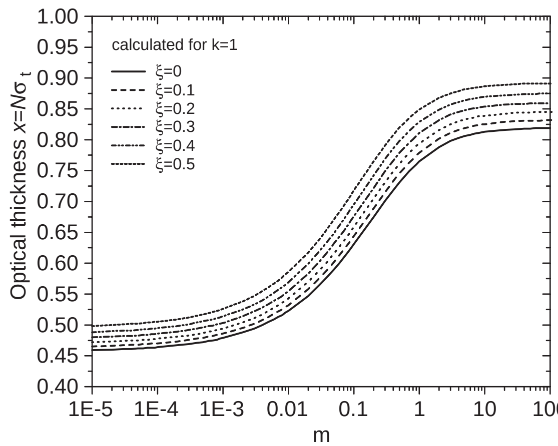

Fig. 3. Optimal optical sample thickness x as a function of the background-to-signal ratio m calculated for different values of the scattering fraction ζ.

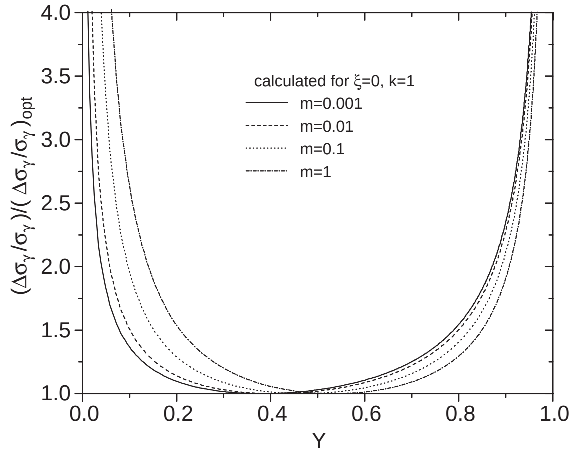

Fig. 4. A calculation of the fractional error in the capture cross-section as a function of the capture yield for several background-to-signal ratios for the case of $k = 1$ and $\xi = 0$.

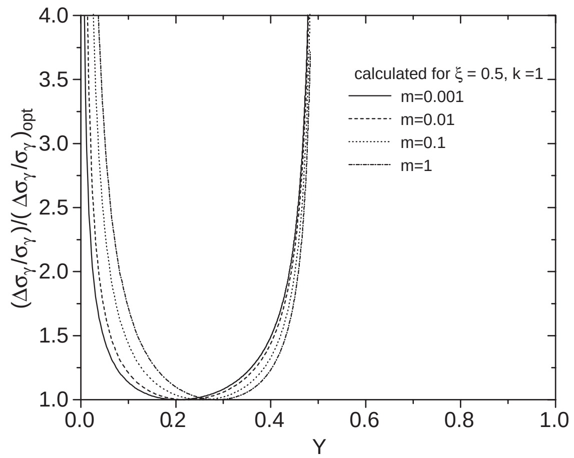

Fig. 5. A calculation of the fractional error in the capture cross-section as a function of the capture yield for several background-to-signal ratios for the case of $k = 1$ and $\xi = 0.5$.

sample with a yield of 0.1 the measured fractional error is increased by a factor of about 2 relative to the fractional error of the optimum sample thickness. In general, the minima in the curves are very shallow and small deviation from the optimum yield results only in a moderate increase in the fractional error of the measured capture cross-section.

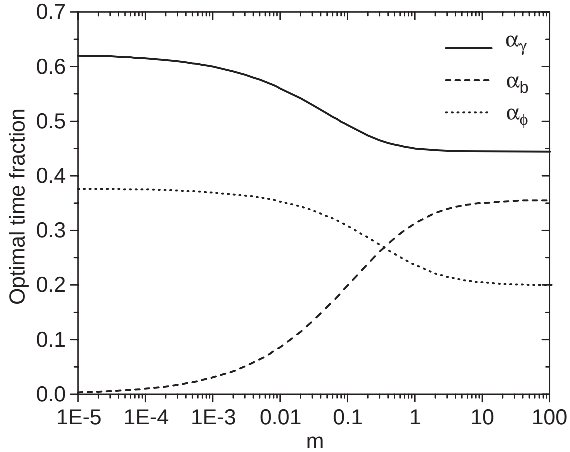

Fig. 6. The optimal time split as a function of the background-to-signal ratio.

To illustrate the effect of scattering on the fractional error, the same calculation was repeated with scattering fraction $\xi = 0.5$ and is shown in Fig. 5. The first observation is that the added scattering reduces the optimum capture yield to values between 0.2 and 0.3. However, the difference from the previous case of $\xi = 0$ is that as the capture yield deviates from the optimum value, the fractional error changes much faster. In such a case there is a much greater "penalty" for using a sample with a thickness that differs significantly from the optimum value.

Finally, the optimum time split was calculated as a function of the background-to-signal ratio and is plotted in Fig. 6. For the case of negligible background, 62% of the total experiment time should be allocated to the sample and the remaining 38% should be allocated to measure the incident neutron rate. As the background-to-signal ratio m increases, more of the experiment time should be allocated to measure the background at the expense of the sample and incident neutron rate times. However, even for the worst case, which is probably not practical, the maximum amount that should be allocated to the background measurement is only 36% of the total time. This type of calculation can be used for capture experiments design. An optimum time split will minimize the error in the measured capture cross-section.

4. Experimental verification

A verification of Eqs. (10)–(12) was done using capture data for natural samarium that was measured at RPI [4]. The data used here are from measurements using metallic samples of samarium with the TOF method. Resonances in the capture cross-section of ^{147}Sm are used because they provide capture cross-section data that varies as a function of the capture yield which is equivalent to variation in the samples optical thickness. The experiment employed a boron carbide overlap filter that absorbs lower energy neutrons that can overlap between pulses. This filter also suppresses the neutron flux below the energy of 10 eV; this provides a change in the background-to-signal ratio in different resonances.

The equations derived in the previous section can be applied to a capture cross-section measured for a sample with optical thickness x. In typical low-energy cross-section measurements, this optical thickness will vary widely in a given resonance. This variation is used to test the equations derived in the previous section.

The first comparison was done with the 3.4 eV resonance. Because of the low energy and the boron carbide overlap filter, the background-to-signal ratio for this resonance is 0.24 which is quite high. This resonance is almost a pure capture resonance with $\xi = 0.0198$, this value can be obtained from the resonance parameters given in Ref. [4] by using the relation $\xi \approx \Gamma_n/(\Gamma_n + \Gamma_\gamma)$ and is varying only by a few percent across the resonance. The flux measurement was done using an enriched ^{10}B sample; however, the detector was configured with only two segments where the capture experiment itself uses 16 segments. This prevents the direct use of the number of neuron pulses to determine the time split for the incident neutron rate α_ϕ. The time fraction α_ϕ was determined by using the ratio between measured count rate and its associated statistical error for a sample $\Delta r_\gamma^2 = r_\gamma/t_\gamma$ and the incident neutron rate $\Delta r_\phi^2 = r_\phi/t_\phi$ which yields $\alpha_\phi/\alpha_s = t_\phi/t_s = r_\phi/r_\gamma \cdot \Delta r_\gamma^2/\Delta r_\phi^2$. The time split for the capture yield and background measurements were determined directly from the number of neutron pulses used in the experiment (which happened to be equal for this case); $\alpha_\gamma = 0.36$, $\alpha_b = 0.36$, $\alpha_\phi = 0.28$. The normalization factor used with this data was $k = 13.6$ and the sample thickness was $N = 7.429 \times 10^{-4}$ atoms/b. To compare the calculation with the experiment, the experimental error was determined using Eq. (6) using the measured data for Y and ΔY. The fractional error in the capture cross-section was calculated using Eq. (10). The two curves were normalized to the fractional error measured or calculated at the optical thickness. This optimal thickness was obtained by minimizing Eq. (10) with respect to x which gave $x_{opt} = 0.37$ that corresponds to $Y_{opt} = 0.3$. The results are plotted in Fig. 7.

This comparison shows good agreement between the experiment and calculations, both exhibit a minimum at the same location and overlap well both below and above the optimum yield. However, the resonance is not strong enough to provide enough points for comparison above the optimum yield. Therefore, another comparison is presented in Fig. 8 with the 18.3 eV resonance which is much stronger, therefore a thinner sample with $N = 3.607 \times 10^{-4}$ atoms/barn was used. This resonance has substantial scattering cross-section with $\xi = 0.515$. Also the background-to-signal ratio in this energy range is much lower; $m = 0.013$. The rest of the

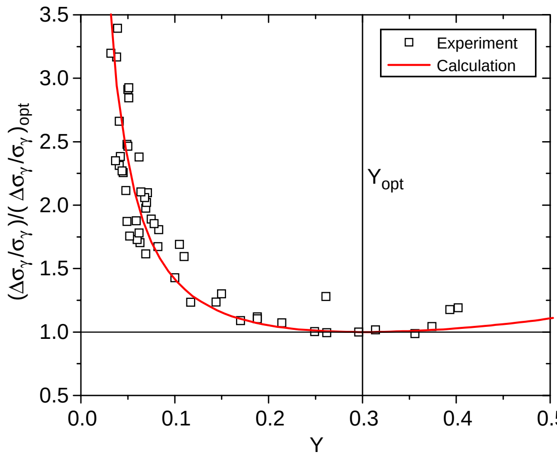

Fig. 7. Comparison of the measured fractional error in the capture cross-section of the 3.4 eV resonance in ^{147}Sm and a calculation using Eq. (10).

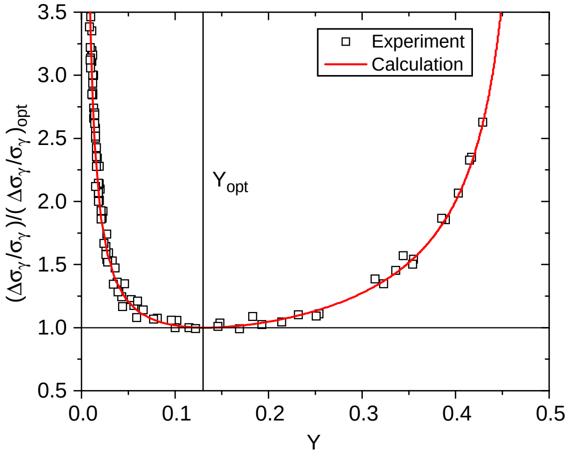

Fig. 8. Comparison of the measured fractional error in the capture cross-section of the 18.3 eV resonance in ^{147}Sm and a calculation using Eq. (10).

parameters are identical to what was used for the 3.4 eV resonance and the same normalization procedure was applied.

The experimental data and calculation are in excellent agreement. This case demonstrates that the optimization procedure shown here can also be used when the measured sample also has about equal amount of scattering and capture. In this case, there is some multiple scattering but it is not high enough to affect the minimization procedure. As expected, in this case, with a smaller background-to-signal ratio, the optimal capture yield $Y_{opt} = 0.13$ is lower than the previous example.

5. Conclusions

A method to optimize the fractional error in capture cross-section measurements has been presented. This analysis allows optimizing experiments by selecting the appropriate sample thickness and time split between the measured capture, background, and incident neutron rates. To minimize the fractional error, the derived expression for the squared fractional error in the capture cross-section was first minimized with respect to the optimum time split followed by minimization with respect to the sample thickness. This information is useful in order to design capture experiments where a fixed experiment time is available and the method developed here can help determine the optimal time split and sample thickness. However, in order to use these equations, prior knowledge of the total cross-section and the scattering fraction are required. The total cross-section can be obtained from transmission measurements, and the scattering fraction frequently can be determined from previous measurements.

For a background-to-signal ratio of 1/100, and a pure capture sample, the optimum capture yield is about 0.4. The optimum yield is related to the sample thickness by the relation given in Eq. (1). The optimum capture yield also depends on the scattering fraction and it was shown that as this fraction increases the optimum sample thickness increases while the optimum yield decreases.

This type of analysis provides some insight on the parameters affecting the statistical error in capture cross-section measurements. However, this analysis does not provide a complete solution to the case of a resonance where the optical thickness varies widely. It is thus desirable to extend this type of minimization to the treatment of resonance parameter measurements similar to the work shown in Ref. [1]. This is of especial interest for experiment design of capture measurements in the resonance region. Finally, this type of error analysis is also valid for other types of partial cross-section measurements such as fission and scattering where the expression for the measured yield is similar to Eq. (1).

References

[1] Yaron Danon, R.C. Block, Nucl. Instr. and Meth. A 485 (2002) 585.

[2] M.E. Rose, M.M. Shapiro, Phys. Rev. 74 (12) (1948) 7.

[3] R.E. Slovacek, R.C. Block, Y. Danon, C. Werner, G.U. Youk, J.A. Burke, N.J. Drindak, F. Feiner, J.A. Helm, K.W. Seemann, Neutron cross-section measurments at the Rensselaer LINAC, Proceedings Topical Meeting, Advances in Reactor Physics, Knoxville, Tennessee, April 11–15, 1994, vol. II, p. 193, American Nuclear Society, 1994.

[4] G. Leinweber, J.A. Burke, H.D. Knox, N.J. Drindak, D.W. Mesh, W.T. Haines, R.V. Ballad, R.C. Block, R.E. Slovacek, C.J. Werner, M.J. Trbovich, D.P. Barry, T. Sato, Nucl. Sci. Eng. 142 (2002) 1.

[5] N.M. Larson, "Updated Users' Guide for SAMMY: Multilevel *R*-Matrix Fits to Neutron Data Using Bayes' Equations," ORNL/TM-9179 (August 1984), ORNL/TM-9179/R6, May 2003.

[6] M.C. Moxon, J.B. Brisland, REFIT, a Least Squares Fitting Program for Resonance Analysis of Neutron Transmission and Capture Data Computer Code, United Kingdom Atomic Energy Authority, Harwell, 1991.